

Dilaton-Limit Fixed Point in Hidden Local Symmetric Parity Doublet Model

Won-Gi Paeng*

Department of Physics, Hanyang University, Seoul 133-791, Korea

Hyun Kyu Lee†

*Department of Physics, Hanyang University, Seoul 133-791, Korea &
Asia Pacific Center for Theoretical physics, Pohang, Gyeongbuk 790-784, Korea*

Mannque Rho‡

*Institut de Physique Théorique, CEA Saclay, 91191 Gif-sur-Yvette cédex, France &
Department of Physics, Hanyang University, Seoul 133-791, Korea*

Chihiro Sasaki§

Frankfurt Institute for Advanced Studies, D-60438 Frankfurt am Main, Germany

August 15, 2018

Abstract

We study nucleon structure with positive and negative parities using a parity doublet model endowed with hidden local symmetry (HLS) with the objective to probe dense baryonic matter. The model – that we shall refer to as “PDHLS model” for short – allows a chiral-invariant mass of the nucleons unconnected to spontaneously broken chiral symmetry which comes out to be $m_0 \sim 200$ MeV at tree level from fitting to the decay width of the parity doubler, N(1535), to nucleon-pion and nucleon axial coupling $g_A = 1.267$. The presence of a substantial m_0 that remains non-vanishing at chiral restoration presents a deep issue for the origin of the nucleon mass as well as will affect nontrivially the equation of state for dense baryonic matter relevant for compact stars. We construct a chiral perturbation theory at one-loop order and explore the phase structure of the model using renormalization group equations. We find a fixed point that we identify with the “dilaton limit” at which the HLS vector mesons decouple from the nucleons. We suggest that cold baryonic system will flow to this limit either before or at reaching the vector manifestation fixed point of hidden local symmetry theory as density increases toward that of chiral restoration.

*e-mail: wgpaeng0@hanyang.ac.kr

†e-mail: hyunku@hanyang.ac.kr

‡e-mail: mannque.rho@cea.fr

§e-mail: sasaki@fias.uni-frankfurt.de

1 Introduction

In the effort to decipher what happens when hadronic matter is compressed to high density as gravity does in compact stars (or to high temperature as in relativistic heavy ion collisions)¹, hidden local symmetry (HLS) [1, 2] promises to be a powerful and predictive theoretical tool, hitherto more or less unexploited. Hidden local symmetry naturally arises when nonlinear sigma (NL σ) model is extended to the energy scale commensurate with the mass of the vector (ρ, ω) mesons. It can be taken as emergent from the current algebra scale [3] or reduced from string theory via holography [4, 5].

HLS makes certain remarkable predictions that are both simple and unanticipated by other approaches available in the literature. While their validity rests on certain assumptions that await confirmations or refutations by QCD proper or experiments, if valid, their consequences on hadronic matter under extreme conditions could be enormous.

There are two particularly notable predictions that we are concerned with here, both of which have not been made in other models. One is that as the hadronic matter approaches the extreme condition – either high temperature or high density – at which a phase transition takes place from broken to restored chiral symmetry, the vector meson mass m_V (where $V = \rho, \omega$) should scale as [2]

$$m_V^*/m_V \approx \langle \bar{q}q \rangle^* / \langle \bar{q}q \rangle \quad (1.1)$$

where the asterisk denotes in medium – temperature T or density n – and q stands for the chiral quark (massless in the chiral limit). More conjecturally, this relation has been extended to other light-quark mesons, leading to BR scaling [6]. One can also write down a similar scaling for the nucleon [7] if one takes the nucleon in the standard (or “naive”) assignment, that is, anchored on the assumption that the nucleon mass is entirely generated dynamically, i.e., by spontaneous breaking of chiral symmetry.

Another striking prediction that is also quite distinctive from others is on the short-distance properties in nuclear interactions in dense medium. If one implements the trace anomaly of QCD in terms of dilatons into the HLS Lagrangian [8]² that we will refer to as dHLS, and if one makes the reasonable assumption that what is called “dilaton limit” [9] is simulating the approach to chiral restoration in density as will be argued below, then the prediction is that the vector-meson coupling to the nucleon g_{VNN} should get suppressed at high density [10]. As a consequence, we have that as density increases, (1) the repulsive core produced by ω -meson exchanges gets suppressed; (2) the tensor force contributed by the ρ exchange gets also suppressed. These two effects are expected to have a large impact on the EoS for compact stars.

We should, however, note that some, if not all, of the predictions mentioned above that involve fermionic, i.e., nucleonic degrees of freedom, can be modified by the possibility that part of the nucleon mass may not be generated dynamically, as for instance in the case of mirror assignment for the nucleons [11, 12]. This would mean that a part of the mass, say, m_0 , would not vanish up to the chiral restoration point. Such a model would substantially

¹In this paper, we will be mainly concerned with density although we will make references to temperature.

²Note that introducing scalar excitations into the NL σ model and equivalently into HLS has been problematic. Here we rely on the locking of scale symmetry with chiral symmetry as discussed in [8].

modify or even invalidate the BR scaling for the nucleon although it may leave intact the one for mesons.

In fact such a structure is found to arise when skyrmions are put on crystal lattice to simulate dense matter. This is a picture of dense baryonic matter for large N_c at which the crystal structure is justified with the nucleon mass going proportional to N_c . What one finds [13] is that a skyrmion matter at a lower density with $\langle \bar{q}q \rangle^* \neq 0$ and $f_\pi^* \neq 0$ undergoes a phase transition at a higher density $n = n_{1/2} > n_0$ to a matter composed of half-skyrmions with $\langle \bar{q}q \rangle^* = 0$ and $f_\pi^* \neq 0$ ³. In this half-skyrmion phase, the in-medium nucleon mass scales proportionally to f_π^* which does not drop appreciably up to the critical density. This suggests that effectively, there is a non-vanishing m_0 . This means that the in-medium nucleon mass does not follow the scaling of light-quark mesons. A notable consequence of this structure is that above n_0 at, say, $(1.3 - 2.0)n_0$, there is a significant change in the structure of nuclear tensor forces – and hence in the equation of state of compact-star matter. In the presence of both pion and ρ , the tensor forces are given by contributions with opposite signs from the pion exchange and ρ exchange. In medium, however, the ρ contribution – which is repulsive – tends to suppress the attraction due to the pion exchange, stiffening the spin-isospin interactions [14] – which is consistent with nature up to nuclear matter density. However if the scaling of the nucleon mass is modified substantially from Brown-Rho scaling by the presence of a large m_0 , then it turns out that as mentioned above, the ρ tensor gets suppressed at some high density, and the pion tensor starts dominating. This feature is expected to have a drastic impact on the EoS, particularly on the symmetry energy E_{sym} , relevant to compact stars [13].

The objective of this paper is to expose the role of the chiral invariant mass m_0 in the nucleon in the framework of an effective field theory anchored on hidden local symmetry. For this purpose, we construct a parity-doublet model for baryons in a hidden local symmetric setting that we shall refer to as “parity-doublet HLS (PDHLS) model” and study what value of m_0 is allowed by nature. We should stress that at this point, we do not know whether this model captures fully the physics of the half-skyrmion phase where a non-zero m_0 is indicated. This is an issue to be addressed further. In this paper, we will restrict ourselves to phenomenology in the vacuum, namely, at $T = n = 0$, relegating in-medium properties to a later publication. Our estimate of m_0 will be at tree order. We will however look at one-loop RGEs for two-point and three-point functions and establish that the dilaton limit taken in [10] to approach mended symmetry corresponds to a fixed point in the one-loop RGE flow in the standard (or “naive”) assignment and also in the mirror assignment for the baryons. The plan of our paper is as follows: we introduce our Lagrangian with parity doublers in Section 2 and deduce an m_0 from the known phenomenology in matter-free space in Section 3. Analysis of the RGEs and the phase structure with the PDHLS model is made in Section 4. A summary and conclusions are given in Section 5. Detailed expressions are summarized in Appendices.

³ The generalized pion decay constant f_π^* can be saturated by not only $\bar{q}q$ but also some higher-dimension operators, such as a four-quark, which could remain condensed giving $f_\pi^* \neq 0$ whereas $\langle \bar{q}q \rangle$ is suppressed in a phase at high density. We suggest that the half-skyrmion phase is such an example.

2 Hidden Local Symmetry in Parity Doublet Model

In this section we give a brief introduction of a nonlinear chiral Lagrangian based on hidden local symmetry (HLS) [1] and introduce parity doubled nucleons [11, 12]. Here and in what follows, we consider a system with $N_f = 2$.

The 2-flavored HLS Lagrangian is based on a $G_{\text{global}} \times H_{\text{local}}$ symmetry, where $G_{\text{global}} = [SU(2)_L \times SU(2)_R]_{\text{global}}$ is the chiral symmetry and $H_{\text{local}} = [SU(2)_V]_{\text{local}}$ is the HLS. The whole symmetry $G_{\text{global}} \times H_{\text{local}}$ is spontaneously broken to a diagonal $SU(2)_V$. The basic quantities are the HLS gauge boson, V_μ , and two matrix valued variables ξ_L, ξ_R , which are combined in a 2×2 special-unitary matrix $U = \xi_L^\dagger \xi_R$. The transformation property of U under the chiral symmetry is given by

$$U \rightarrow g_L U g_R^\dagger, \quad (2.1)$$

with $g_{L,R} \in [SU(2)_{L,R}]_{\text{global}}$. The variables ξ s transform as

$$\xi_{L,R} \rightarrow h \xi_{L,R} g_{L,R}^\dagger, \quad (2.2)$$

with $h \in [SU(2)_V]_{\text{local}}$, and are parameterized as

$$\xi_{L,R} = e^{i\sigma/F_\sigma} e^{\mp i\pi/F_\pi}, \quad (2.3)$$

where $\pi = \pi^a T_a$ denotes the pseudoscalar Nambu-Goldstone (NG) bosons associated with the spontaneous symmetry breaking of G_{global} chiral symmetry, and $\sigma = \sigma^a T_a$ denotes the NG bosons associated with the spontaneous breaking of H_{local} . The σ is absorbed into the HLS gauge boson through the Higgs mechanism and the gauge boson acquires its mass. F_π and F_σ are the decay constants of the associated particles. The HLS gauge field transforms as

$$V_\mu \rightarrow ih\partial_\mu h^\dagger + hV_\mu h^\dagger. \quad (2.4)$$

The fundamental objects are the Maurer-Cartan 1-forms defined by

$$\begin{aligned} \hat{\alpha}_\perp^\mu &= \frac{1}{2i} \left[D^\mu \xi_R \cdot \xi_R^\dagger - D^\mu \xi_L \cdot \xi_L^\dagger \right], \\ \hat{\alpha}_\parallel^\mu &= \frac{1}{2i} \left[D^\mu \xi_R \cdot \xi_R^\dagger + D^\mu \xi_L \cdot \xi_L^\dagger \right], \end{aligned} \quad (2.5)$$

which transform homogeneously:

$$\hat{\alpha}_{\perp,\parallel}^\mu \rightarrow h \hat{\alpha}_{\perp,\parallel}^\mu h^\dagger. \quad (2.6)$$

The covariant derivatives of $\xi_{L,R}$ are given by

$$\begin{aligned} D_\mu \xi_L &= \partial_\mu \xi_L - iV_\mu \xi_L + i\xi_L \mathcal{L}_\mu, \\ D_\mu \xi_R &= \partial_\mu \xi_R - iV_\mu \xi_R + i\xi_R \mathcal{R}_\mu, \end{aligned} \quad (2.7)$$

with \mathcal{L}_μ and \mathcal{R}_μ being the external gauge fields introduced by gauging G_{global} . The Lagrangian with the lowest derivatives is given by [2]

$$\mathcal{L}_M = F_\pi^2 \text{tr} [\hat{\alpha}_{\perp\mu} \hat{\alpha}_\perp^\mu] + F_\sigma^2 \text{tr} [\hat{\alpha}_{\parallel\mu} \hat{\alpha}_\parallel^\mu] - \frac{1}{2g^2} \text{tr} [V_{\mu\nu} V^{\mu\nu}], \quad (2.8)$$

where g is the HLS gauge coupling and the field strengths are defined by $V_{\mu\nu} = \partial_\mu V_\nu - \partial_\nu V_\mu - i[V_\mu, V_\nu]$. Expanding $\hat{\alpha}_{\perp\mu}$ and $\hat{\alpha}_{\parallel\mu}$,

$$\hat{\alpha}_{\perp}^{\mu} = \frac{1}{F_{\pi}} \partial_{\mu} \pi + \mathcal{A}^{\mu} - \frac{1}{F_{\pi}} [\mathcal{V}^{\mu}, \pi] - \frac{1}{6F_{\pi}^3} [[\partial_{\mu} \pi, \pi], \pi] + \dots, \quad (2.9)$$

$$\hat{\alpha}_{\parallel}^{\mu} = \frac{1}{F_{\sigma}} \partial_{\mu} \sigma + \mathcal{V}^{\mu} - V^{\mu} - \frac{i}{2F_{\pi}^2} [\partial_{\mu} \pi, \pi] - \frac{i}{F_{\pi}} [\mathcal{A}^{\mu}, \pi] + \dots, \quad (2.10)$$

where $\mathcal{V}^{\mu} = (\mathcal{R}^{\mu} + \mathcal{L}^{\mu})/2$ and $\mathcal{A}^{\mu} = (\mathcal{R}^{\mu} - \mathcal{L}^{\mu})/2$, one finds the vector meson mass and the $\rho\pi\pi$ coupling constant as

$$m_V^2 = ag^2 F_{\pi}^2, \quad a = \frac{F_{\sigma}^2}{F_{\pi}^2}, \quad (2.11)$$

$$g_{\rho\pi\pi} = \frac{1}{2} ag. \quad (2.12)$$

The Lagrangian of mirror nucleons in the non-linear realization without vector mesons was considered in [15]. Its HLS-extended form is found to be [10]

$$\begin{aligned} \mathcal{L}_N = & \bar{Q} i \gamma^{\mu} D_{\mu} Q - g_1 F_{\pi} \bar{Q} Q + g_2 F_{\pi} \bar{Q} \rho_3 Q \\ & - i m_0 \bar{Q} \rho_2 \gamma_5 Q + g_V \bar{Q} \gamma^{\mu} \hat{\alpha}_{\parallel\mu} Q + g_A \bar{Q} \rho_3 \gamma^{\mu} \hat{\alpha}_{\perp\mu} \gamma_5 Q, \end{aligned} \quad (2.13)$$

where the nucleon doublet $Q = \begin{pmatrix} Q_1 \\ Q_2 \end{pmatrix}$ transforms as

$$Q \rightarrow h Q, \quad (2.14)$$

the covariant derivative $D_{\mu} = \partial_{\mu} - i V_{\mu}$, the ρ_i are the Pauli matrices acting on the parity-doublet and g_A and g_V are dimensionless parameters. To diagonalize the mass term in Eq. (2.13), we transform Q into a new field N :

$$\begin{pmatrix} N_+ \\ N_- \end{pmatrix} = \frac{1}{\sqrt{2 \cosh \delta}} \begin{pmatrix} e^{\delta/2} & \gamma_5 e^{-\delta/2} \\ \gamma_5 e^{-\delta/2} & -e^{\delta/2} \end{pmatrix} \begin{pmatrix} Q_1 \\ Q_2 \end{pmatrix}, \quad (2.15)$$

where $\sinh \delta = -\frac{g_1 F_{\pi}}{m_0}$. We identify N_{\pm} as parity even and odd states respectively. The nucleon masses are found to be

$$m_{N_{\pm}} = \mp g_2 F_{\pi} + \sqrt{(g_1 F_{\pi})^2 + m_0^2}, \quad (2.16)$$

$$\cosh \delta = \frac{m_{N_+} + m_{N_-}}{2m_0}. \quad (2.17)$$

Finally, we arrive at the Lagrangian in the parity eigenstate as

$$\mathcal{L}_N = \bar{N} i \not{D} N - \bar{N} \hat{\mathcal{M}} N + g_V \bar{N} \gamma^{\mu} \hat{\alpha}_{\parallel\mu} N + g_A \bar{N} \gamma^{\mu} \hat{G} \hat{\alpha}_{\perp\mu} \gamma_5 N, \quad (2.18)$$

$$\hat{\mathcal{M}} = \begin{pmatrix} m_{N_+} & 0 \\ 0 & m_{N_-} \end{pmatrix}, \quad \hat{G} = \begin{pmatrix} \tanh \delta & \gamma_5 / \cosh \delta \\ \gamma_5 / \cosh \delta & -\tanh \delta \end{pmatrix}. \quad (2.19)$$

The axial couplings for nucleons are

$$g_{AN_+N_+} = -g_{AN_-N_-} = g_A \tanh \delta. \quad (2.20)$$

3 Chiral Invariant Mass of the Nucleon

In this section, we calculate the decay width of $N_- \rightarrow \pi N_+$ to extract the mass parameter m_0 and calculate the pion-nucleon scattering lengths to be compared with the experimental data.

3.1 Decay width of $N_- \rightarrow N_+ + \pi$

The decay width at tree is given by

$$\Gamma = C_2(r) \frac{(m_{N_-} - m_{N_+})^2}{8\pi F_\pi^2} \sqrt{(m_{N_-} - m_{N_+})^2 - m_\pi^2} \left(\frac{g_A}{\cosh \delta} \right)^2 \frac{[(m_{N_-} + m_{N_+})^2 - m_\pi^2]^{\frac{3}{2}}}{2m_{N_-}^3}, \quad (3.1)$$

with $C_2(r) = T^a T_a = \frac{3}{4}$ in SU(2). The nucleon axial-coupling in a linear sigma model for the parity doublers and pions, given by $g_{AN_+N_+} = g_A \tanh \delta$, is typically smaller than unity. In order to recover the well established experimental value, 1.267, one should add more states, in particular the $\Delta(1232)$ isobar, so that the Adler-Weisberger sum rule is saturated by those resonances [11].

In a non-linear sigma model, on the other hand, g_A can be an arbitrary parameter in Eq. (2.13) to be determined from the constraint,

$$g_{AN_+N_+} = g_A \tanh \delta = 1.267. \quad (3.2)$$

Using the experimental values of $F_\pi = 92.42$ MeV, $m_{N_+} = 939$ MeV, $m_{N_-} = 1535$ MeV, one obtains the decay width as a function of m_0^4 as in Fig. 1. Using the decay width [16],

$$\Gamma_{N_- \rightarrow N_+ \pi}^{\text{exp}} = 70 \pm 26.25 \text{ MeV}, \quad (3.3)$$

we get a bound of m_0 as

$$m_0 = 204 \pm 39 \text{ MeV}. \quad (3.4)$$

This corresponds to

$$0.981 \lesssim \tanh \delta \lesssim 0.991. \quad (3.5)$$

3.2 πN scattering lengths

The pion-nucleon scattering amplitude, $\pi^a(q) + N(p) \rightarrow \pi^b(q') + N(p')$, is written as

$$T^{ab}(p, q; p', q') = \bar{u}(p') \left[\left(A^{(+)} + \frac{1}{2} (\not{q} + \not{q}') B^{(+)} \right) \delta_{ab} + \left(A^{(-)} + \frac{1}{2} (\not{q} + \not{q}') B^{(-)} \right) i\epsilon_{bac} \tau_c \right] u(p),$$

⁴Since $\left(\frac{g_A}{\cosh \delta} \right)^2 = g_A^2 (\tanh \delta)^2 \left(\frac{1}{1 - \frac{4m_0^2}{(m_{N_+} + m_{N_-})^2}} - 1 \right)$, setting $g_A \tanh \delta = 1.267$, one finds that only ' m_0 ' remains as the undetermined parameter.

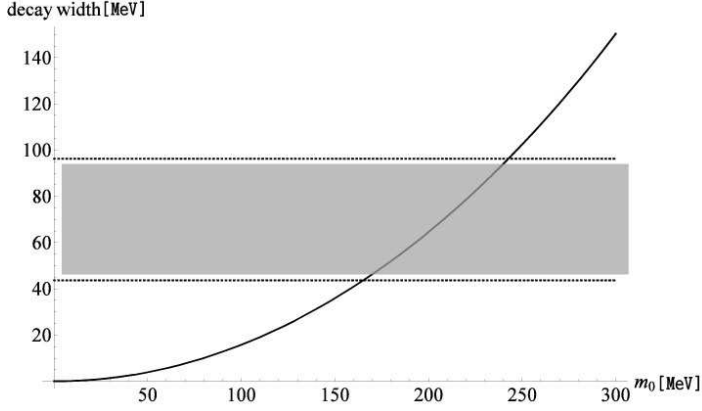


Figure 1: Decay width of $N_- \rightarrow N_+\pi$. The gray colored region describes the experimental bound [16].

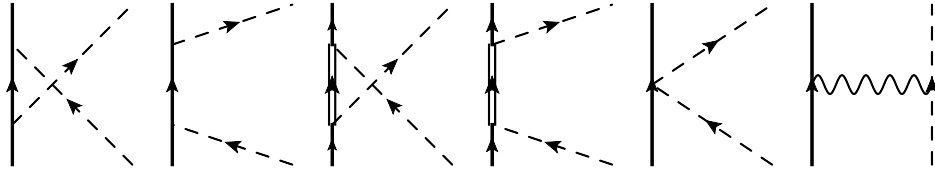


Figure 2: Diagrams relevant to πN scattering lengths at the tree level. The solid, dashed, double and wiggled lines describe nucleon, pion, parity partner of the nucleon and ρ meson respectively.

where a and b are isospin indices. The s-wave isospin-even and isospin-odd scattering lengths are defined in terms of the Mandelstam variables as

$$a_0^{(\pm)} = \frac{1}{4\pi (1 + m_\pi/m_{N_+})} \left(A_0^{(\pm)} + m_\pi B_0^{(\pm)} \right), \quad (3.6)$$

where the subscript 0 indicates that we take $s = (m_{N_+} + m_\pi)^2$, $t = 0$ and $u = (m_{N_+} - m_\pi)^2$. The tree diagrams contributing to the scattering lengths are shown in Fig. 2. Using the Feynman rules obtained from the Lagrangians (2.8) and (2.18), one arrives at the following

expressions:

$$a_0^+ = \frac{1}{4\pi \left(1 + \frac{m_\pi}{m_{N_+}}\right)} \left\{ - \left(\frac{g_A}{F_\pi} \tanh \delta \right)^2 \frac{m_{N_+} m_\pi^2}{4m_{N_+}^2 - m_\pi^2} + \left(\frac{g_A}{F_\pi} \frac{1}{\cosh \delta} \right)^2 \frac{m_\pi^2 (m_{N_-} - m_{N_+})}{2 \left((m_{N_-} - m_{N_+})^2 - m_\pi^2 \right)} \right\}, \quad (3.7)$$

$$a_0^- = \frac{1}{4\pi \left(1 + \frac{m_\pi}{m_{N_+}}\right)} \left\{ \left(\frac{g_A}{F_\pi} \tanh \delta \right)^2 \frac{m_\pi^3}{2 \left(4m_{N_+}^2 - m_\pi^2 \right)} + \left(\frac{g_A}{F_\pi} \frac{1}{\cosh \delta} \right)^2 \frac{m_\pi^3}{2 \left[(m_{N_-} - m_{N_+})^2 - m_\pi^2 \right]} + g_V \frac{m_\pi}{2F_\pi^2} + (1 - g_V) \frac{m_\pi a g^2}{2m_\rho^2} \right\}. \quad (3.8)$$

We note that in the last line of Eq. (3.8) the terms with g_V are precisely canceled since $m_\rho^2 = a g^2 F_\pi^2$. This means that the contribution from $NN\pi\pi$ interaction is canceled and ρ meson interaction gives the main contribution to the odd scattering length. This cancellation arises independently of any HLS parameters and therefore it is purely the consequence of low-energy theorems of chiral symmetry. Since the nonlinear sigma model (NL σ M) is gauge-equivalent to HLS, all low-energy theorems of the NL σ M are encoded in the HLS Lagrangian [1]. The baryon HLS Lagrangian constructed here has the HLS and hence has the same low-energy theorems of the baryonic NL σ M.

Using Eq. (3.4) for m_0 , we obtain the scattering lengths

$$a_0^+ = (-6.0 \pm 0.4) \times 10^{-5} \text{MeV}^{-1}, \quad (3.9)$$

$$a_0^- = (57 \pm 1) \times 10^{-5} \text{MeV}^{-1}, \quad (3.10)$$

which are to be compared the experimental values[17],

$$a_{0,\text{exp}}^+ = (-2.446 \pm 0.504) \times 10^{-5} \text{MeV}^{-1}, \quad a_{0,\text{exp}}^- = (66.043 \pm 0.935) \times 10^{-5} \text{MeV}^{-1}. \quad (3.11)$$

Considering that these are tree-order results, they are not unreasonable. The discrepancy from the experimental data could be removed if other resonances, such as, e.g., the axial-vector mesons are included as in [18].

3.3 m_0 in various models

In this section, we compare the values of m_0 evaluated in the various approaches summarized in Table 1.

- **m_0 in vacuum**

The chiral invariant mass, m_0 , can be determined solely from the decay width of $N(1535)$ to π and $N(940)$ in a linear sigma model without axial-vector mesons. For

	m_0 [MeV]	$\rho(\mathbf{770})$	$a_1(\mathbf{1260})$
LSM (tree) [11]	270	no	no
LSM (tree) [18]	460 ± 136	yes	yes
HBChPT (1-loop) [15]	335 ± 95	no	no
this work (tree)	204 ± 39	yes	no

Table 1: The range of m_0 extracted in various approaches in medium-free space. “LSM” stands for linear sigma model and “HBChPT” for heavy baryon chiral perturbation theory, respectively.

the experimental value for the width $\Gamma \simeq 70$ MeV, the model predicts $m_0 \simeq 270$ MeV [11, 18]. However the pion-nucleon scattering lengths and the axial charges calculated in the model do not come out in agreement with the existing data. In particular, the isospin-even scattering length depends strongly on the sigma-meson mass that cannot be pinned down accurately.

In order to have a better fit, one introduces the axial-vector meson a_1 in such a way that it couples to the positive-parity nucleon differently from the negative-parity state, as well as an independent coupling strength of the vector (axial-vector) mesons to the nucleons [18]. The free parameters can be varied to reproduce the experimental data $\Gamma_{N_- \rightarrow N_+ \pi} = 67.5 \pm 23.6$ MeV, $\Gamma_{a_1 \rightarrow \pi \gamma} = 0.640 \pm 0.246$ MeV and $g_{AN_+N_+} = 1.267 \pm 0.004$, and the lattice measurement, $g_{AN_-N_-}^{\text{lattice}} = 0.2 \pm 0.3$ [19]⁵. The model also gives the π -N scattering lengths in reasonable agreement with experiments [18].

Using a three-flavor heavy-baryon chiral Lagrangian [20], one-loop chiral perturbation calculation for widths was carried out for various channels [15]. Within the given experimental uncertainties that reflect on the parameters of the Lagrangian, the m_0 extracted is found to range $240 \text{ MeV} \lesssim m_0 \lesssim 430 \text{ MeV}$. Here the error comes mainly from a large uncertainty of the decay width of $N^* \rightarrow \pi N$. The corresponding range of $\tanh \delta$ in the width increases due to the loop corrections and thus m_0 becomes slightly smaller than its tree-level value.

- **m_0 in hot and dense matter:**

The linear sigma model with parity doublers has been applied to symmetric [21, 22, 23] and asymmetric nuclear matter [24] in hot and dense environment within mean field approximation. The model is constructed in such a way that at $T = 0$ the properties of nuclear matter, i.e. saturation, binding energy and incompressibility, are correctly reproduced while satisfying low-energy theorems of chiral symmetry. In order to have a reasonable value for incompressibility, a large $m_0 \sim 800$ MeV is found to be required. This is substantially changed when a scalar tetraquark-state is introduced, which makes the incompressibility in an acceptable range with $m_0 \sim 500$ MeV [25].

A different approach to determine m_0 has recently been proposed using a chiral Lagrangian implementing conformal invariance, where the origin of m_0 is mostly of the gluon condensate. With the chiral symmetry restoration temperature taken to be

⁵It is perhaps unsafe to rely on the sole measurement available for this quantity if the prediction is sensitive to its value. Further lattice measurements are needed.

$T_{\chi\text{SR}} \sim 170$ MeV, at zero density, the m_0 comes out to be ~ 210 MeV [10]. This coincides with the result of the HLS model at tree obtained in this paper, Eq. (3.4).

As stressed in Introduction, both the dilaton scalar and the vector mesons in dHLS are the relevant degrees of freedom in nuclear matter and could lead in the mean-field approximation to a better treatment of both nuclear matter and matter at higher density, thereby giving a better constraint on m_0 than so far arrived at, i.e., ~ 500 -800 MeV. This work is presently being done and will be a subject of future publication.

4 Analysis of Renormalization Group Equations

The phase structure of the HLS model has been studied based on the renormalization group equations (RGEs) where loop effects are systematically calculated using the chiral perturbation theory including vector mesons at one-loop order [2]. HLS renders a systematic chiral perturbation feasible in the presence of the vector mesons. The key point is that the HLS coupling constant can be taken as

$$g \sim \mathcal{O}(p), \quad (4.1)$$

which means that the vector meson mass is of $\mathcal{O}(p)$, in the same chiral order as the pion mass. With the vector meson mass ~ 6 times the pion mass in matter-free space, this counting may appear to be unreasonable but it is justified by that it goes as $\mathcal{O}(N_c^0)$ with the corrections coming at $\mathcal{O}(1/N_c)$ and is endowed with the vector manifestation fixed point of HLS at which the vector meson mass goes to zero in the chiral limit. In fact it has been shown in [2] that chiral perturbation expansion works even in matter-free space as well as does nonlinear sigma model at one-loop order to which the HLS expansion has been done. We will take this as an indication that the extrapolation from large N_c to $N_c = 3$ is a reliable approximation. In this section we further extend it to a system with parity-doubled nucleons. We will follow closely the quantization procedure of Ref. [2]. Details of the diagrammatic calculations and the RGEs are relegated to Appendices A and B. In this section we analyze the RGEs and their fixed-point structure of the hidden local symmetric parity-doublet model.

In order to gain insight, it is helpful to examine the standard (or “naive”) assignment with $m_0 = 0$. The details are given in Appendix A. Here we summarize the key results of the analysis.

The four coupled equations (A.2), (A.3), (A.4) and (A.5) describe the RGE flows of the masses $m_{N_{\pm}}$ and coupling constants g_A and $(1 - g_V)$. It is a complicated set of equations and has not yet been fully analyzed. There may be several fixed points or fixed lines. There is however one strikingly simple fixed point which is easy to identify and is argued to be relevant to QCD and that is what is called “dilaton-limit fixed point (DLFP for short)” corresponding to the dilaton limit discussed in [10]:

$$(1 - g_V, g_A - g_V, M_S, M_D) = (0, 0, 0, 0) \quad (4.2)$$

where $M_S = \frac{1}{4}(m_{N_+} + m_{N_-})^2$ and $M_D = \frac{1}{4}(m_{N_+} - m_{N_-})^2$. This ensures that the vector mesons decouple from the nucleons toward the dilaton limit encoded by $g_A = g_V = 1$ and the suppression of the repulsive force due to the vector meson exchange [10] remains a robust

statement at the quantum level. In fact, the DLFP is an infrared fixed point, i.e.,

$$\frac{\partial}{\partial M_D} \left[\mu \frac{dM_D}{d\mu} \right] = 6 \left(\frac{1}{4\pi F_\pi} \right)^2 \mu^2 > 0, \quad (4.3)$$

$$\frac{\partial}{\partial M_S} \left[\mu \frac{dM_S}{d\mu} \right] = 6 \left(\frac{1}{4\pi F_\pi} \right)^2 \mu^2 > 0, \quad (4.4)$$

$$\frac{\partial}{\partial (1 - g_V)} \left[\mu \frac{d(1 - g_V)}{d\mu} \right] = \frac{1}{(4\pi F_\sigma)^2} [(3 - a^2 + 2a) \mu^2 + m_\rho^2] > 0, \quad (4.5)$$

$$\frac{\partial}{\partial g_A} \left[\mu \frac{dg_A}{d\mu} \right] = \frac{4}{(4\pi F_\pi)^2} \mu^2 > 0, \quad (4.6)$$

for which we set $(1 - g_V, g_A - g_V, M_S, M_D) = (0, 0, 0, 0)$. A special value $a = 2$ explains the vacuum phenomenology, such as the vector meson dominance, although it is not a fixed point of the RGE. The HLS theory possesses $a = 1$ as a fixed point matching with QCD taking $\langle \bar{q}q \rangle \rightarrow 0$ [2] and this is not affected by the nucleons when $M_D = M_S = 0$. Thus, Eq. (4.6) is always positive for any a in the range between 1 and 2.

Now turning to the case of the mirror assignment with $m_0 \neq 0$, the situation is a bit more involved since the treatment will depend upon whether m_0 is light or heavy: Consider two extreme limits: (1) $m_0 \sim \mathcal{O}(m_\pi)$ and (2) $m_0 \gg \Lambda_{\text{QCD}}$. In the case (1), we can treat m_0 as the small quantity as one does in ChPT and ignore terms of $\mathcal{O}(m_0)$ and then the above analysis will apply. In the case of (2), we apply heavy-baryon formalism as one does in heavy-baryon chiral perturbation theory (HBChPT). As in HBChPT, $\mathcal{O}(m_0^{-1})$ is ignored. For details, see Appendix B. It is verified that the coupled equations do possess the infrared fixed point and the dilaton-limit fixed point is intact for both cases of $m_0 \approx 0$ and $m_0 \gg \Lambda_{\text{QCD}}$,

$$(1 - g_V, g_V - g_A, M_S, M_D) = (0, 0, m_0^2, 0), \quad (4.7)$$

as in the standard assignment.

The suppressed repulsive interaction associated with an IR fixed point is therefore a common feature in the two different assignments, “naive” and mirror, of chirality. It is natural that the short-distance interaction is independent of the chirality assignment. The physics behind it must be related with some new symmetries which may dynamically emerge in hot/dense matter. We consider that this is a manifestation of “emergent symmetry” akin to that associated with the Harada-Yamawaki vector manifestation in hidden local symmetry [2]. As shown in [10], at the dilaton limit the lowest-lying mesons (scalar, pseudo-scalar, vector and axial-vector) are assembled into a full representation of chiral group. Weinberg’s mended symmetry [26] – which is not present in the fundamental QCD Lagrangian but can be emergent due to in-medium collective excitations – becomes manifest there and this might protect the dilaton limit at quantum level. We note that this aspect of emergence of symmetries, both for the dilaton-limit fixed point and the vector manifestation fixed point, is absent in the approaches found in the literature that are not anchored on hidden flavor gauge symmetry and represents a falsifiable bona-fide prediction of HLS in dense and hot matter.

5 Remarks and Conclusions

In this paper, we constructed a parity-doublet nonlinear sigma model with hidden local symmetry (PDHLS model) and extracted at the lowest order in chiral perturbation theory the chiral-invariant mass m_0 from experimental data in the vacuum. We found it to be ~ 200 MeV. By itself, this value has little significance, since in nonlinear realization, the chiral-invariant mass m_0 gets compounded into the physical mass with important dynamically generated mass. Furthermore, quantum loop corrections may not be ignored in the analysis. However it turns out to play an important role in dense baryonic matter as discussed in [10] and re-stressed below.

In calculating quantum loop corrections in the PDHLS model (the detailed discussion of the results of which will be relegated to a future publication), we have discovered that the one-loop renormalization group equations (RGE) have a fixed point that has not been so far observed in other approaches. The set of four coupled equations for the RGE flow of the nucleon masses $m_{N\pm}$, the vector coupling g_V and the axial-vector coupling g_A have a simple IR fixed point $(1 - g_V, g_A - g_V, M_S, M_D) = (0, 0, m_0^2, 0)$ in the standard (with $m_0 = 0$) or mirror (with $m_0 \neq 0$) assignment. It is very possible that these set of equations possess a variety of other fixed points, some of which may be consistent with QCD. Our proposal here is that this fixed point that we refer to as dilaton-limit fixed point (DLFP) is precisely the “dilaton limit” considered in [10] that encodes the phenomenon of mended symmetries [26].

As discussed in [10], one way of driving the baryonic system at zero temperature and low density ($n \lesssim n_0$) described by the HLS (or PDHLS) Lagrangian to a dense baryonic system ($n \gg n_0$) is to introduce a scalar degree of freedom in HLS (or PDHLS) in terms of the “soft” dilaton associated with the trace anomaly of QCD and then take the dilaton limit [9] to go over to the linearly realized (Gell-Mann-Lévy-type) sigma model Lagrangian. This dilaton limit is found to correspond exactly to the DLFP we found in the RGEs described above.⁶ We interpret this exact correspondence as implying that as density increases toward that of chiral restoration, the dense matter flows toward this fixed point, the import of that point being that the vector-meson–nucleon coupling gets suppressed at high density. The major consequence of this fixed point is that the strong hard-core repulsion present in nuclear interactions (aptly described in terms of ω exchanges between two or more nucleons) and the ρ tensor force contributing crucially to the symmetry energy in neutron-rich systems as in compact stars will be strongly suppressed. How this prediction will affect the equation of state for compact stars is a very important issue to be worked out.

An intriguing possibility that can be entertained here is that the DLFP and the vector manifestation fixed point (VM) of HLS [2] may be intricately linked. In HLS, the fixed point $(a, g) = (1, 0)$ gets linked to QCD via the matching of QCD current correlators at the matching scale by identifying the $\langle \bar{q}q \rangle \rightarrow 0$ limit with the HLS coupling $g \rightarrow 0$ limit. We conjecture that the DLFP linked to conformal symmetry is an IR fixed point that is reached *before* the VM/HLS is reached. This is quite analogous to the limit $a \rightarrow 1$ before reaching the “vector limit” $g = 0$ as Georgi discussed for vector symmetry in HLS [27]. Unlike in the case of the VM/HLS where the matching of correlators enables one to make contact with QCD,

⁶Although a heuristic consideration indicates that the fixed point is robust, we have not however verified in detail that this fixed point remains unaffected when the dilaton field χ is introduced into the loop diagrams. The basic problem here is that scalar fields of the χ type are problematic in higher order calculations.

here we are not making any direct “match” with QCD. We are assuming that the dilaton limit imposed on effective field theory which works well at the low density commensurate with nuclear matter is consistent with the phase structure of QCD at high density where chiral phase transition is to take place. As stated, we cannot rule out the possibility that the set of our RGEs have other fixed points that are not inconsistent with QCD. This issue will be an object of future study.

Now a comment on the role of a non-zero chiral invariant mass m_0 in nuclear physics. When nuclear matter is described in effective field theory anchored on the low-momentum nuclear interaction V_{low-k} derived via Wilsonian renormalization group equations, how the nucleon mass scales in medium as a function of density turns out to be quite important for the structure of finite nuclei as well as nuclear matter [28, 29]. The presence of a substantially big m_0 as is found in some analysis in medium [22] would affect crucially how the nucleon mass scales in density in such effective field theory approach to nuclei, nuclear matter and dense compact-star matter.

Acknowledgments

We acknowledge partial support by the WCU project of the Korean Ministry of Educational Science and Technology (R33-2008-000-10087-0). Part of this work was done when three of us (WGP, HKL and MR) were participating in the WCU-YITP Molecule Collaboration 18 April-18 May 2011. The work of C.S. has been partly supported by the Hessian LOEWE initiative through the Helmholtz International Center for FAIR (HIC for FAIR).

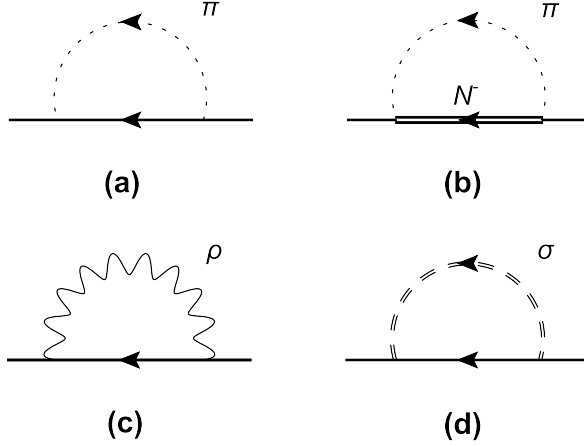


Figure 3: Diagrams of the nucleon self-energy: the thin solid line corresponds to the nucleon and the double line to its odd-parity partner.

APPENDIX

A Chiral Perturbation Theory in the Standard Assignment

Consider the standard (or “naive”) assignment with $m_0 = 0$. In the strict $m_0 = 0$ limit, the parity doublet decouple but here we take a non-zero m_0 and set it equal to zero at the end. This exercise allows us to gain some insight into what happens in the mirror scenario for the case when m_0 is small. We will consider the system to be near chiral restoration and assume that the entire mass of the nucleons is generated by spontaneous chiral symmetry breaking, with $m_{N_{\pm}}$ vanishing at its restoration point. We can then assign the chiral counting $\mathcal{O}(p)$ to the mass:

$$m_{N_{\pm}} \sim \mathcal{O}(p). \quad (\text{A.1})$$

Evaluating the one-loop diagrams Fig. 3 in the relativistic formalism, one finds the RGEs of the nucleon masses as

$$\begin{aligned} \mu \frac{dM_D}{d\mu} &= \frac{3g_A^2}{8\pi^2 F_\pi^2} M_D [\mu^2 - M_D - 3M_S] \\ &\quad - \frac{9(1-g_V)^2}{16\pi^2} g^2 M_D, \end{aligned} \quad (\text{A.2})$$

$$\begin{aligned} \mu \frac{dM_S}{d\mu} &= \frac{3g_A^2}{8\pi^2 F_\pi^2} M_S (\mu^2 - M_S - 3M_D) \\ &\quad - \frac{9(1-g_V)^2}{16\pi^2} g^2 M_S, \end{aligned} \quad (\text{A.3})$$

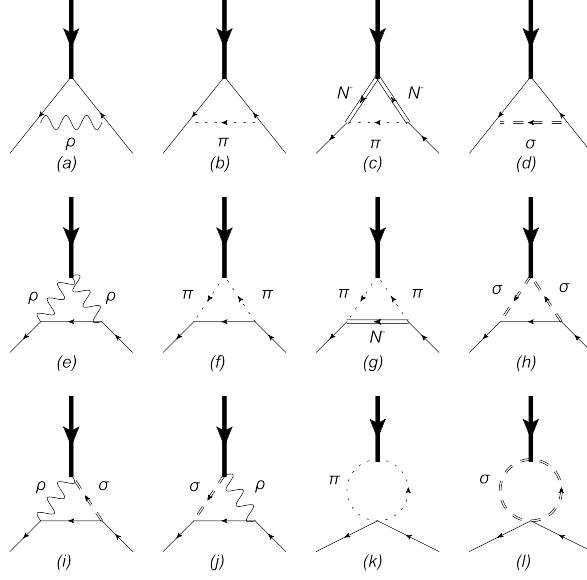


Figure 4: One-loop diagrams contributing to the $\bar{V}N_+N_+$ three-point function.

which indicate the dynamically generated masses vanish at the fixed point. The RGEs of the Yukawa couplings from Figs. 4-6, in the $m_0 \rightarrow 0$ limit, are obtained as

$$\mu \frac{d}{d\mu} (1 - g_V) = \frac{m_{N_+}^2}{8\pi^2 F_\pi^2} \tilde{\mathcal{F}}_0 + (1 - g_V) \frac{1}{8\pi^2} \tilde{\mathcal{F}}_1 + (g_V - g_A^2) \frac{1}{8\pi^2} \tilde{\mathcal{F}}_2, \quad (\text{A.4})$$

$$\mu \frac{dg_A}{d\mu} = \frac{m_{N_+}^2 g_A}{8\pi^2 F_\pi^2} \tilde{\mathcal{G}}_0 + (1 - g_V) \frac{g_A}{8\pi^2} \tilde{\mathcal{G}}_1 + (g_V - g_A^2) \frac{g_A}{8\pi^2} \tilde{\mathcal{G}}_2, \quad (\text{A.5})$$

where m_{N_+} becomes zero when $M_D = 0$ and $M_S = 0$. It is easy to see that $(1 - g_V, g_A - g_V, M_S, M_D) = (0, 0, 0, 0)$ is the fixed point of the coupled RGEs. The explicit expressions of $\tilde{\mathcal{F}}_i$ and $\tilde{\mathcal{G}}_i$ are given by

$$\begin{aligned} \tilde{\mathcal{F}}_0 &= \frac{1}{4} \left(ag_A^2 + \frac{g_V^2}{a} \right), \\ \tilde{\mathcal{F}}_1 &= \left[\frac{g_A^2}{F_\pi^2} + \frac{g_V(1+2g_V)}{2F_\sigma^2} \right] \mu^2 - \frac{3}{2} \left(\frac{g_A^2}{F_\pi^2} + \frac{g_V^2}{F_\sigma^2} \right) m_{N_+}^2 + g^2 \left(2 - \frac{3}{2} g_V \right), \\ \tilde{\mathcal{F}}_2 &= \frac{a}{2F_\pi^2} \mu^2, \end{aligned} \quad (\text{A.6})$$

$$\begin{aligned} \tilde{\mathcal{G}}_0 &= \frac{1}{4} \left(g_A^2 + \frac{g_V^2}{a} + 2g_V \right), \\ \tilde{\mathcal{G}}_1 &= \left(\frac{2}{F_\pi^2} + \frac{1-g_V}{F_\sigma^2} \right) \mu^2 + \frac{2g_V}{F_\sigma^2} m_{N_+}^2 - \frac{5}{2} ag^2, \\ \tilde{\mathcal{G}}_2 &= -\frac{1}{F_\pi^2} \left(\mu^2 - 2m_{N_+}^2 \right). \end{aligned} \quad (\text{A.7})$$

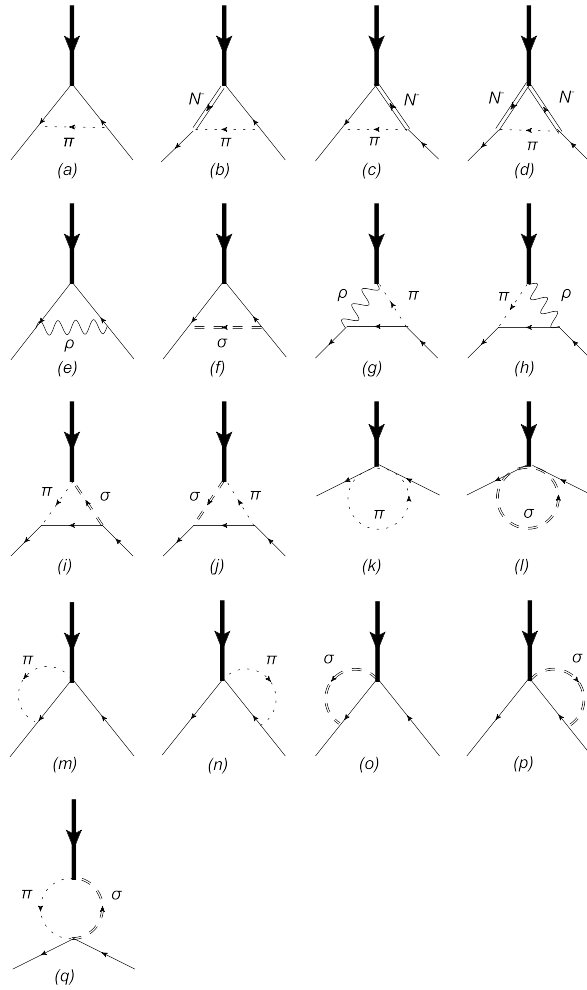


Figure 5: One-loop diagrams contributing to the $\bar{A}N_+N_+$ vertex.

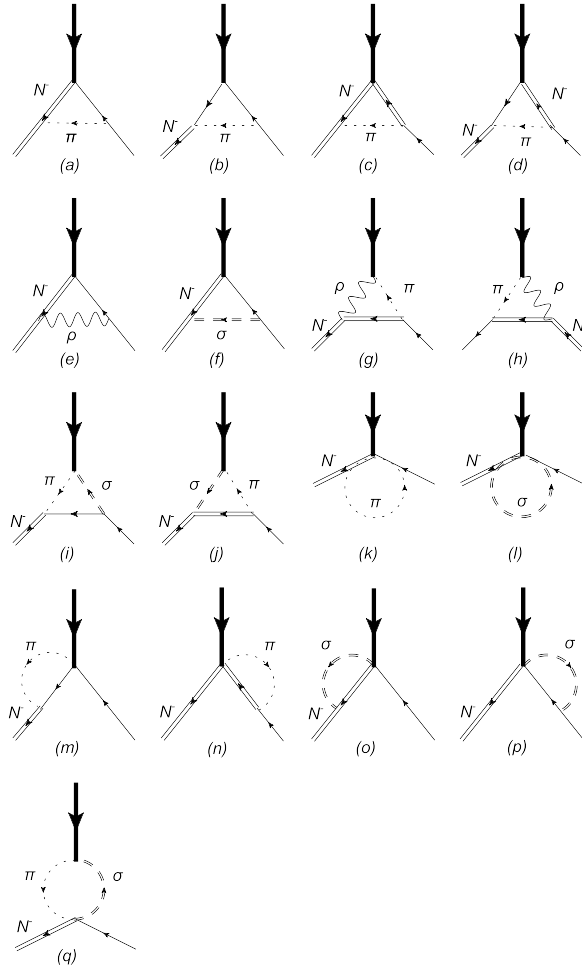


Figure 6: One-loop diagrams contributing to the $\bar{A}N_-N_+$ vertex.

The RGEs of F_π^2 , a and g are obtained as

$$\mu \frac{dF_\pi^2}{d\mu} = \frac{1}{(4\pi)^2} [3a^2 g^2 F_\pi^2 + 2(2-a)\mu^2] - \frac{g_A^2}{2\pi^2} (m_{N_+}^2 + m_{N_-}^2), \quad (\text{A.8})$$

$$\mu \frac{da}{d\mu} = -\frac{1}{(4\pi)^2} (a-1) \left[3a(1+a)g^2 - (3a-1)\frac{\mu^2}{F_\pi^2} \right] + \frac{g_A^2}{2\pi^2} \frac{a}{F_\pi^2} (m_{N_+}^2 + m_{N_-}^2), \quad (\text{A.9})$$

$$\mu \frac{dg^2}{d\mu} = -\frac{1}{(4\pi)^2} \frac{87-a^2}{6} g^4 + \frac{1}{6\pi^2} (1-g_V)^2 g^4, \quad (\text{A.10})$$

which agree with the expressions given in [7] when the nucleons are replaced with constituent quarks.

B Chiral Perturbation Theory in the Mirror Assignment

In the mirror assignment the nucleon mass is not entirely generated by spontaneous chiral symmetry breaking and we identify the origin of the chiral invariant mass m_0 with the explicit breaking of the QCD scale invariance, i.e. a hard dilaton [10], which has no direct link with the chiral dynamics. Consider m_0 to be large compared with dynamically generated mass and adopt a heavy baryon chiral perturbation theory (HBChPT) [30] in the presence of m_0 . We write the nucleon momentum as

$$p^\mu = m_0 v^\mu + k^\mu, \quad (\text{B.1})$$

where v^μ is the four-velocity with $v^2 = 1$ and k^μ is the residual momentum of order Λ_{QCD} , so that one can perform a chiral perturbation theory systematically in energy range below the chiral symmetry breaking scale $\Lambda_\chi \sim 1$ GeV. A heavy baryon field B is defined by ⁷

$$\begin{pmatrix} B_+ \\ B_- \end{pmatrix} = \exp [im_0 v \cdot x] \begin{pmatrix} N_+ \\ N_- \end{pmatrix}. \quad (\text{B.2})$$

The Lagrangian (2.18) is rewritten as ⁸

$$\begin{aligned} \mathcal{L}_N &= i\bar{B}v^\mu D_\mu B - \Delta m_+ \bar{B}_+ B_+ - \Delta m_- \bar{B}_- B_- \\ &\quad + g_V \bar{B}v^\mu \hat{\alpha}_{\parallel\mu} B + g_A \bar{B} \left(2S^\mu \rho_3 \tanh \delta + v^\mu \rho_1 \frac{1}{\cosh \delta} \right) \hat{\alpha}_{\perp\mu} B, \end{aligned} \quad (\text{B.3})$$

where S^μ is the spin operator and

$$\Delta m_\pm = m_{N_\pm} - m_0. \quad (\text{B.4})$$

Note that because of the reduction (B.2) two small scales comparable to Λ_{QCD} , Δm_\pm , appear in the mass term.

For our calculation in the background field gauge, we again follow the notations of Harada and Yamawaki [2] for quantum and background fields. In case of without a negative parity nucleon, further details can be found in, e.g. [31].

⁷ This is a slightly different definition from that introduced in [15].

⁸ In HBChPT in the mirror assignment, we treat $\frac{p}{m_0}$ as a small quantity. We calculate the two- and three-point functions with the Lagrangian (B.3) and obtain the RGEs for M_S , M_D , $1-g_V$ and g_A . Then, we take the leading order terms of $\mathcal{O}\left(\frac{p^2}{(4\pi F_\pi)^2}\right)$ and drop the terms of $\mathcal{O}\left(\frac{p^2}{(4\pi F_\pi)^2} \left(\frac{p}{m_0}\right)^n\right)$ with $n \geq 1$ after expanding $\tanh^2 \delta$, $\frac{1}{\cosh^2 \delta}$ and Δm_\pm^2 in $\frac{p}{m_0}$.

B.1 Quantum corrections to the Yukawa couplings

In this subsection, we show the $\bar{V}B_+B_+$ three-point functions and give the regularization condition for $(1 - g_V)$, where \bar{V}_μ is the background field of the HLS gauge field V_μ . The renormalized coupling is given by

$$(1 - g_V)_{\text{bare}} = Z_{3V} \left(Z_N Z_V^{1/2} \right)^{-1} (1 - g_V), \quad (\text{B.5})$$

where Z_V represents the wavefunction renormalization of the vector field and Z_{3V} appears in the counter term of the vector interaction. Expanding $Z_{N,3V} = 1 + Z_{N,3V}^{(1)} \cdots$ and using $Z_V = 1$ for the classical field \bar{V}^μ , one obtains the regularization condition as

$$(1 - g_V)_{\text{bare}} + (1 - g_V) \left(-Z_{3V}^{(1)} + Z_N^{(1)} \right) = \text{finite}. \quad (\text{B.6})$$

The counter terms are calculated from the 1-loop graphs of the two- and three-point functions:

$$Z_{3V}^{(1)} = \Gamma_{\bar{V}B_+B_+} |_{\text{div}} / (1 - g_V), \quad (\text{B.7})$$

where the $\Gamma_{\bar{V}B_+B_+}$ is the sum of 1-loop diagrams given in Fig. 4.

Other relevant three-point functions which give the loop corrections to the axial coupling g_A are the $\bar{A}B_+B_+$ and $\bar{A}B_+B_-$ functions. The 1-loop graphs are shown in Figures 5 and 6.

The renormalization conditions read

$$(g_A \tanh \delta)_{\text{bare}} + g_A \tanh \delta \left(-Z_{3A++}^{(1)} + Z_{N_+}^{(1)} \right) = \text{finite}, \quad (\text{B.8})$$

and

$$\left(\frac{g_A}{\cosh \delta} \right)_{\text{bare}} + \frac{g_A}{\cosh \delta} \left[-Z_{3A+-}^{(1)} + \frac{1}{2} \left(Z_{N_+}^{(1)} + Z_{N_-}^{(1)} \right) \right] = \text{finite}, \quad (\text{B.9})$$

with

$$Z_{3A++}^{(1)} = \Gamma_{\bar{A}B_+B_+} |_{\text{div}} / (g_A \tanh \delta), \quad Z_{3A+-}^{(1)} = \Gamma_{\bar{A}B_+B_-} |_{\text{div}} / (g_A / \cosh \delta). \quad (\text{B.10})$$

B.2 Renormalization group equations for the 2- and 3-point functions

In the ordinary HBChPT without a negative parity nucleon, the leading order parameters, m_N and g_A , are not renormalized in the chiral limit. In the present perturbation theory with the reduction (B.2), Δm_\pm appears as the small scales which remain non-vanishing in the chiral limit. Therefore, the nucleon masses and coupling constants receive loop corrections proportional to Δm_\pm . Using the standard technique to evaluate the loop integrals [31], one obtains the RGE of M_D as

$$\mu \frac{dM_D}{d\mu} = 6 \left(\frac{g_A}{4\pi F_\pi \cosh \delta} \right)^2 M_D (\mu^2 + 8M_D), \quad (\text{B.11})$$

whereas M_S does not evolve with the loop effect at this order, i.e.

$$\mu \frac{dM_S}{d\mu} = 0. \quad (\text{B.12})$$

The $\bar{A}B_+B_+$ and $\bar{A}B_+B_-$ functions computed from Figs. 5 and 6 give the RGEs of $g_A \tanh \delta$ and $g_A/\cosh \delta$. Using the identity,

$$\mu \frac{d}{d\mu} \left(\frac{g_A^2}{\cosh^2 \delta} \right) + \mu \frac{d}{d\mu} (g_A^2 \tanh^2 \delta) = \mu \frac{d}{d\mu} (g_A^2), \quad (\text{B.13})$$

the RGE of g_A is derived. From Eqs.(B.6), (B.8) and (B.9), one arrives at the RGEs of $(1 - g_V)$ and g_A :

$$\mu \frac{d}{d\mu} (1 - g_V) = \frac{1}{8\pi^2} \mathcal{F}_0 + (1 - g_V) \frac{1}{8\pi^2} \mathcal{F}_1 + (g_V - g_A^2) \frac{1}{8\pi^2} \mathcal{F}_2, \quad (\text{B.14})$$

$$\mu \frac{dg_A}{d\mu} = \frac{g_A}{8\pi^2} \mathcal{G}_0 + (1 - g_V) \frac{g_A}{8\pi^2} \mathcal{G}_1 + (g_V - g_A^2) \frac{g_A}{8\pi^2} \mathcal{G}_2, \quad (\text{B.15})$$

where \mathcal{F}_i and \mathcal{G}_i are functions of the parameters, F_π, a, g, g_A, g_V and m_{N_\pm} . The functions \mathcal{F}_0 and \mathcal{G}_0 are given by

$$\mathcal{F}_0 = \frac{ag_A^2}{F_\pi^2} \left[(\mu^2 + 3\Delta m_+^2) \tanh^2 \delta + \frac{\Delta m_-^2}{\cosh^2 \delta} \right] + \frac{g_V^2}{F_\sigma^2} \Delta m_+^2, \quad (\text{B.16})$$

$$\begin{aligned} \mathcal{G}_0 = & \left(-\frac{g_A^2}{F_\pi^2 \cosh^2 \delta} + \frac{2g_V}{F_\pi^2} \right) \mu^2 \tanh^2 \delta + \frac{3g_A^2}{4F_\pi^2 \cosh^2 \delta} \left(\Delta m_+^2 + \Delta m_-^2 + \frac{2}{3} \Delta m_+ \Delta m_- \right) \\ & + \frac{g_A^2}{F_\pi^2} \tanh^2 \delta \left[4\Delta m_+^2 \tanh^2 \delta - \frac{1}{\cosh^2 \delta} (\Delta m_+^2 - 2\Delta m_-^2 + \Delta m_+ \Delta m_-) \right] \\ & + \frac{g_V^2}{F_\sigma^2} \left[2\Delta m_+^2 \tanh^2 \delta + \frac{3}{4 \cosh^2 \delta} \left(\Delta m_+^2 + \Delta m_-^2 + \frac{2}{3} \Delta m_+ \Delta m_- \right) \right] \\ & - \frac{g_V}{F_\pi^2} \left[2\Delta m_+^2 \tanh^2 \delta - \frac{1}{\cosh^2 \delta} (\Delta m_+^2 + \Delta m_-^2) \right], \end{aligned} \quad (\text{B.17})$$

and therefore vanish when $(M_S, M_D) = (m_0^2, 0)$ whereas $\mathcal{F}_{1,2}$ and $\mathcal{G}_{1,2}$ remain non-vanishing in this choice of parameters. Expanding $\tanh^2 \delta$, $\frac{1}{\cosh^2 \delta}$ and Δm_\pm^2 in $\frac{1}{m_0}$, the RGEs, (B.11), (B.12), (B.14) and (B.15), are given in the leading order of $\frac{1}{m_0}$ by

$$\mu \frac{dM_D}{d\mu} = \frac{3g_A^2}{8\pi^2 F_\pi^2} M_D (\mu^2 + 8M_D) \left[1 + \mathcal{O} \left(\frac{1}{m_0^2} \right) \right], \quad (\text{B.18})$$

$$\mu \frac{dM_S}{d\mu} = 0, \quad (\text{B.19})$$

$$\mu \frac{d}{d\mu} (1 - g_V) = \left[\frac{M_D}{8\pi^2 F_\pi^2} \bar{\mathcal{F}}_0 + \frac{(1 - g_V)}{8\pi^2} \bar{\mathcal{F}}_1 + \frac{(g_V - g_A^2)}{8\pi^2} \bar{\mathcal{F}}_2 \right] \left[1 + \mathcal{O} \left(\frac{1}{m_0} \right) \right], \quad (\text{B.20})$$

$$\mu \frac{dg_A}{d\mu} = \left[\frac{M_D g_A}{8\pi^2 F_\pi^2} \bar{\mathcal{G}}_0 + (1 - g_V) \frac{g_A}{8\pi^2} \bar{\mathcal{G}}_1 + (g_V - g_A^2) \frac{g_A}{8\pi^2} \bar{\mathcal{G}}_2 \right] \left[1 + \mathcal{O} \left(\frac{1}{m_0} \right) \right], \quad (\text{B.21})$$

where $\bar{\mathcal{F}}_i$ and $\bar{\mathcal{G}}_i$ are given by

$$\begin{aligned}
\bar{\mathcal{F}}_0 &= ag_A^2 + \frac{g_V^2}{a}, \\
\bar{\mathcal{F}}_1 &= \left[\frac{g_A^2}{F_\pi^2} + \frac{g_V(1+2g_V)}{2F_\sigma^2} \right] \mu^2 + 6M_D \left(\frac{g_A^2}{F_\pi^2} + \frac{g_V^2}{F_\sigma^2} \right) \\
&\quad - g^2 \left(4 - \frac{15}{2}g_V + 3g_V^2 \right), \\
\bar{\mathcal{F}}_2 &= \frac{a}{2F_\pi^2} \mu^2, \\
\bar{\mathcal{G}}_0 &= g_A^2 + \frac{g_V^2}{a} + 2g_V, \\
\bar{\mathcal{G}}_1 &= \left(\frac{2}{F_\pi^2} + \frac{1-g_V}{F_\sigma^2} \right) \mu^2 - \frac{4g_V}{F_\sigma^2} M_D \\
&\quad - g^2 \left[3(1-g_V) + \frac{5}{2}a \right], \\
\bar{\mathcal{G}}_2 &= -\frac{1}{F_\pi^2} (\mu^2 + 4M_D),
\end{aligned} \tag{B.22}$$

$$\bar{\mathcal{G}}_2 = -\frac{1}{F_\pi^2} (\mu^2 + 4M_D), \tag{B.23}$$

and all terms in the RGEs are $\mathcal{O}\left(\frac{p^2}{(4\pi F_\pi)^2}\right)$ in chiral counting. With Eqs. (B.18), (B.19), (B.20) and (B.21), we arrive at the fixed point $(1-g_V, g_A-g_V, M_S, M_D) = (0, 0, m_0^2, 0)$ in the large m_0 limit.

References

- [1] M. Bando, T. Kugo, S. Uehara, K. Yamawaki and T. Yanagida, Phys. Rev. Lett. **54**, 1215 (1985), M. Bando, T. Kugo and K. Yamawaki, Phys. Rept. **164**, 217 (1988).
- [2] M. Harada and K. Yamawaki, Phys. Rept. **381**, 1 (2003).
- [3] D.T. Son and M.A. Stephanov, Phys. Rev. **D69**, 065020 (2004).
- [4] T. Sakai and S. Sugimoto, Prog. Theor. Phys. **113**, 843 (2005). Prog. Theor. Phys. **114**, 1083 (2005).
- [5] M. Harada, S. Matsuzaki and K. Yamawaki, Phys. Rev. D **82**, 076010 (2010).
- [6] G. E. Brown and M. Rho, Phys. Rev. Lett. **66**, 2720 (1991).
- [7] M. Harada, Y. Kim and M. Rho, Phys. Rev. D **66**, 016003 (2002).
- [8] H. K. Lee and M. Rho, Nucl. Phys. A **829**, 76 (2009).
- [9] S. R. Beane and U. van Kolck, Phys. Lett. B **328**, 137 (1994).
- [10] C. Sasaki, H. K. Lee, W. G. Paeng and M. Rho, Phys. Rev. D **84**, 034011 (2011).
- [11] C. E. Detar and T. Kunihiro, Phys. Rev. D **39**, 2805 (1989).

- [12] D. Jido, Y. Nemoto, M. Oka and A. Hosaka, Nucl. Phys. A **671**, 471 (2000), D. Jido, T. Hatsuda and T. Kunihiro, Phys. Rev. Lett. **84**, 3252 (2000), D. Jido, M. Oka and A. Hosaka, Prog. Theor. Phys. **106**, 873 (2001).
- [13] H. K. Lee, B. Y. Park and M. Rho, Phys. Rev. C **83**, 025206 (2011).
- [14] G. E. Brown and M. Rho, Phys. Lett. B **237**, 3 (1990).
- [15] Y. Nemoto, D. Jido, M. Oka and A. Hosaka, Phys. Rev. D **57**, 4124 (1998).
- [16] K. Nakamura *et al.* [Particle Data Group], J. Phys. G **37**, 075021 (2010).
- [17] S. R. Beane, V. Bernard, E. Epelbaum, U. G. Meissner and D. R. Phillips, Nucl. Phys. A **720**, 399 (2003). U. G. Meissner, U. Raha and A. Rusetsky, Phys. Lett. B **639**, 478 (2006).
- [18] S. Gallas, F. Giacosa and D. H. Rischke, Phys. Rev. D **82**, 014004 (2010).
- [19] T. T. Takahashi and T. Kunihiro, Phys. Rev. D **78**, 011503 (2008).
- [20] E. E. Jenkins, A. V. Manohar, Phys. Lett. **B255**, 558-562 (1991).
- [21] T. Hatsuda and M. Prakash, Phys. Lett. B **224**, 11 (1989).
- [22] D. Zschiesche, L. Tolos, J. Schaffner-Bielich and R. D. Pisarski, Phys. Rev. C **75**, 055202 (2007).
- [23] C. Sasaki and I. Mishustin, Phys. Rev. C **82**, 035204 (2010).
- [24] V. Dexheimer, S. Schramm and D. Zschiesche, Phys. Rev. C **77**, 025803 (2008), V. Dexheimer, G. Pagliara, L. Tolos, J. Schaffner-Bielich and S. Schramm, Eur. Phys. J. A **38**, 105 (2008).
- [25] S. Gallas, F. Giacosa and G. Pagliara, “Nuclear matter within a dilatation-invariant parity doublet model: the role of the tetraquark at nonzero density,” arXiv:1105.5003 [hep-ph].
- [26] S. Weinberg, Phys. Rev. Lett. **65**, 1177 (1990).
- [27] H. Georgi, Nucl. Phys. B **331**, 311 (1990).
- [28] L. W. Siu, J. W. Holt, T. T. S. Kuo and G. E. Brown, Phys. Rev. C **79**, 054004 (2009).
- [29] D. Dong, T.T.S. Kuo, H.K. Lee and M. Rho, to appear.
- [30] E. E. Jenkins, A. V. Manohar, Phys. Lett. **B255**, 558-562 (1991).
- [31] T. -S. Park, D. -P. Min, M. Rho, Phys. Rept. **233**, 341-395 (1993).